

**Exactly soluble model of resonant energy transfer between molecules**C. King,<sup>1,\*</sup> B. Barbiellini,<sup>2</sup> D. Moser,<sup>1,2</sup> and V. Renugopalakrishnan<sup>3,4</sup><sup>1</sup>*Department of Mathematics, Northeastern University, Boston, Massachusetts 02115, USA*<sup>2</sup>*Department of Physics, Northeastern University, Boston, Massachusetts 02115, USA*<sup>3</sup>*Children's Hospital, Harvard Medical School, Boston, Massachusetts 02115, USA*<sup>4</sup>*Department of Chemistry and Chemical Biology, Northeastern University, Boston, Massachusetts 02115, USA*

(Received 11 April 2011; published 7 March 2012)

Förster's theory of resonant energy transfer (FRET) predicts the strength and range of exciton transport between separated molecules. We introduce an exactly soluble model for FRET which reproduces Förster's results as well as incorporating quantum coherence effects. As an application, the model is used to analyze a system composed of quantum dots and the protein bacteriorhodopsin.

DOI: [10.1103/PhysRevB.85.125106](https://doi.org/10.1103/PhysRevB.85.125106)

PACS number(s): 33.90.+h, 42.50.Dv, 87.14.E-, 87.64.K-

**I. INTRODUCTION**

It has long been known that near-field electrodynamics allows energy transfer without emission of real photons. A striking example of this principle is provided by recent advances in wireless nonradiative energy transfer;<sup>1</sup> another recent example is Auger-mediated "sticking,"<sup>2</sup> whereby scattering states of positrons may transition to bound states in a metal, by transferring energy to a valence electron which can then leave the surface of the metal. Nowadays the phenomenon of nonradiative decay is of great scientific interest in many different fields of physics and chemistry.<sup>3</sup> In particular, new paradigms for solar energy conversion make use of nonradiative coupling for direct transfer of energy from the excitons created in the solar absorber to high-mobility charge carriers.<sup>4,5</sup> The mechanism for this transfer relies on the near-field resonance of electric dipoles and is generally known as Förster resonance energy transfer (FRET).<sup>6-8</sup> In its simplest formulation, FRET<sup>9</sup> is the quantum version of a classical resonance phenomenon, whereby oscillating electric dipoles exchange energy through their mutual electric fields.<sup>10</sup> Some studies in the quantum version have considered the possibility of coherent interactions between the dipoles.<sup>11-18</sup> Such quantum coherence has been observed in the FMO complex,<sup>21</sup> and it has been suggested that this may partly explain the high efficiency of energy transfer between chromophores. Interestingly, it has recently been demonstrated that the classical dipole model can reproduce the effects of quantum coherence as well.<sup>19,20</sup> In this work, we revisit the analysis of the rate and efficiency of FRET, in the context of a donor and an acceptor species with comparable electronic energy gaps. In this situation FRET is evidenced by decreased natural fluorescence from the donor and enhanced fluorescence from the acceptor. The distance over which FRET has been observed ranges from 1 to 10 nm, with the strength varying as the inverse sixth power of the separation.

The fundamental mechanism underlying FRET is resonance between excited electronic states in the donor and the acceptor molecules. The excited electronic states have nonzero electric dipole moments, and the resulting dipoles experience a Coulomb interaction. The energy exchange is complicated by the coupling of electronic states to vibronic molecular states, leading to a broadening of the linewidths and a weakening of the resonant interaction. This vibronic coupling explains

the difference between early inaccurate calculations of FRET efficiency (by Perrin<sup>10</sup> and others), which were based solely on dipole resonance, and the later, more successful calculations by Förster,<sup>8</sup> which included vibronic effects.

In this paper we consider a simple model for FRET which incorporates both electronic and vibronic effects. The model applies in situations where the donor molecule is rigid, with weak coupling between its electronic and its vibronic states, while the acceptor has strong electronic-vibronic coupling in its excited state. In this situation the model is exactly solvable and thus allows a comparison with the perturbative formulas derived by Förster and others. In particular, we derive exact formulas for FRET efficiency and the Förster radius, and we compare these to the well-known Förster formulas. Furthermore, the model is fully quantum mechanical and predicts coherent oscillations between donor and acceptor under strong FRET conditions. The model contains a parameter which determines the strength of the electronic-vibronic coupling in the acceptor, and for weak coupling the model reproduces the long-range interactions (up to 100 nm) calculated by Perrin.<sup>10</sup>

As described above, the model applies to a FRET system where a rigid donor species, with weak coupling between electronic and vibronic states, interacts with an acceptor species where electronic and vibronic states are strongly coupled. Thus the donor is modeled by a simple two-state system, corresponding to its electronic ground and excited states. The donor's vibronic degrees of freedom are "frozen" and do not appear in the model. As we discuss in more detail below, this kind of model can be realized in practice with quantum dots (QDs). For the acceptor we again include only two electronic states, corresponding to the ground and excited states, but in addition, we include vibronic effects in the excited state. The excited band is described in detail below. For the moment, we note that the electronic-vibronic coupling is derived from the Born-Oppenheimer approximation and assumes that the vibronic degrees of freedom are entrained to the electronic state. Initially we assume that the vibronic degrees of freedom are also frozen in the acceptor ground state. Later we indicate how nonzero temperature effects may be included by unfreezing these degrees of freedom.

The key step in the solution of our model is the reduction to a finite-dimensional system which exhibits the same efficiency

for resonant energy transfer. The efficiency can be computed exactly for this finite-dimensional model, and this provides our exact results for the full model. In order to compare with Förster's formulas, we also compute the absorption coefficient for our model, and we use this to evaluate the overlap integral which appears in the standard rate formulas.

As an application we apply our model to the analysis of one particular system of this type which exhibits FRET, namely, the pairing of a QD donor species with bacteriorhodopsin (bR) as the acceptor. The QD is known to have sharp emission lines for fluorescence and, thus, is a good candidate for the "rigid" donor molecule described above. We find good agreement with other calculations of the FRET rate for this system.

## II. DESCRIPTION OF THE MODEL

We employ the Born-Oppenheimer approximation and assume that the electronic state of the molecule determines its overall character, so that the vibronic state is entrained to the electronic state. Thus the state space is a direct sum  $\mathcal{H}_0 \oplus \mathcal{H}_1 \oplus \dots$ , with one factor for each electronic state. The electronic configuration determines an effective Hamiltonian for the vibronic degrees of freedom, and each space  $\mathcal{H}_k$  is spanned by these vibronic states attached to the corresponding electronic state. The spaces  $\mathcal{H}_k$  may be discrete or continuous, depending on the structure of the vibronic states. For simplicity, we include only two electronic states, the ground state and the excited state, thus the state space is  $\mathcal{H}_{\text{gr}} \oplus \mathcal{H}_{\text{exc}}$ .

### A. The ground subspace $\mathcal{H}_{\text{gr}}$

We assume a nondegenerate electronic ground state  $|\psi_{\text{gr}}\rangle$ , and we also assume that the vibronic modes are frozen, so  $\mathcal{H}_{\text{gr}}$  is one-dimensional. For the acceptor this assumes zero temperature. Later we extend to nonzero temperatures by including vibronic ground states.

### B. The excited subspace $\mathcal{H}_{\text{exc}}$

Again, we assume a nondegenerate electronic excited state  $|\psi_{\text{exc}}\rangle$ . For the donor, the vibronic modes are frozen, so that  $\mathcal{H}_{\text{exc}}$  is one-dimensional. However, for the acceptor, the electronic state determines an effective Hamiltonian for the vibronic states, which are labeled by their energy eigenvalues  $\varepsilon$ . For this subspace we assume that the vibronic states form a continuous band with a uniform density of states, with eigenvalues extending from  $-\infty$  to  $+\infty$ . Under this assumption we ignore any edge effects in the band. Thus the space  $\mathcal{H}_{\text{exc}}$  is isomorphic to the one-particle Hilbert space  $L^2(\mathbb{R})$ , and we represent a state as a square integrable function  $\phi_{\text{exc}}(\varepsilon)$  where

$$\int_{-\infty}^{\infty} |\phi_{\text{exc}}(\varepsilon)|^2 d\varepsilon = 1. \quad (1)$$

The time evolution is  $\phi_{\text{exc}}(\varepsilon) \rightarrow e^{-i\varepsilon t} \phi_{\text{exc}}(\varepsilon)$ . For convenience we denote the Hamiltonian in this basis as  $h$ , so that

$$(h\phi_{\text{exc}})(\varepsilon) = \varepsilon\phi_{\text{exc}}(\varepsilon). \quad (2)$$

## C. Excitons

As long as the electronic state does not change, the dynamics of the vibronic state is completely determined by the fixed effective Hamiltonian corresponding to this electronic configuration (here we are neglecting any feedback reaction from the vibronic modes on the electronic modes). However, when the molecule undergoes an electronic transition, for example, by photon absorption, the effective Hamiltonian for the vibronic states immediately changes. This sudden change creates an excited vibronic state, as the previously stationary vibronic state becomes a superposition of energy eigenstates of the new Hamiltonian. We call this vibronic state an *exciton*. The exciton behaves like a delocalized one-particle state. In our model, exciton states will arise only in the excited band of the acceptor, due to a transition from the ground state. We assume an average energy  $E_3$  for these exciton states.

## D. Transitions

Turning now to transitions, we consider only radiative interactions which act solely on the electronic state. Thus transitions of the vibronic state occur as a consequence of the change of the effective Hamiltonian due to the electronic transition. The electronic matrix element due to the interaction  $V$  is

$$\langle \psi_{\text{exc}} | V | \psi_{\text{gr}} \rangle. \quad (3)$$

We find an explicit form for this matrix element for the situations of interest, namely, direct photon absorption and resonant excitation through the Coulomb interaction. In order to determine the vibronic matrix element, we follow Jortner<sup>22</sup> and proceed by analogy with the derivation of the lineshape of a resonance. Recall that a resonance is a perturbation of an embedded eigenvalue in continuous spectrum. The perturbation causes the eigenvalue to "dissolve," accompanied by the emission of a one-particle state in the continuous spectrum. In our model this one-particle state is the exciton. Thus the transition from a vibronic ground state is accompanied by the creation of an exciton, which is a normalized excited vibronic state. The Breit-Wigner form for the lineshape of the resonance is a Lorentzian, where the width corresponds to the lifetime of the resonance,<sup>22</sup> and the center is the average energy. We assume the same form for the exciton, so the wave function of the exciton (in the diagonal energy representation) is the square root of a Lorentzian:

$$f(\varepsilon) = \sqrt{\frac{\gamma}{2\pi}} \frac{e^{i\theta}}{(\varepsilon - E_3) + \frac{i}{2}\gamma}. \quad (4)$$

Using a Lorentzian form implicitly assumes that the energy band extends from  $-\infty$  to  $+\infty$ . We make this assumption, thus ignoring any edge effects in the band. The width  $\gamma$  depends on the particular system and determines the lifetime of the exciton. The Lorentzian is centered at energy  $E_3$ , corresponding to the average exciton energy. We also include a phase factor  $e^{i\theta}$ , which may depend on  $\varepsilon$ . As we will see, this phase factor is irrelevant to the calculation of the FRET efficiency.

## III. DYNAMICS OF THE MODEL

The FRET interaction between the donor and the acceptor causes an exchange of energy as the excited state is transferred from one to the other. Although the transfer becomes

irreversible after some time, the initial interaction is unitary and thus admits the possibility of oscillations between donor and acceptor.

We use standard notation, with  $D$  for donor ground state,  $D^*$  for donor excited state,  $A$  for acceptor ground state, and  $A^*$  for acceptor excited state. Thus the coupled donor-acceptor system is described by the collection of states

$$|DA\rangle, |D^*A\rangle, |DA^*\rangle, |D^*A^*\rangle, \quad (5)$$

where both  $|DA\rangle$  and  $|D^*A\rangle$  are single states, while  $|DA^*\rangle$  and  $|D^*A^*\rangle$  contain the exciton subspace.

### A. The Hamiltonian

The FRET interaction is dipole-dipole in lowest order, and so its strength decays as the inverse third power of the distance. The Hamiltonian is determined by the matrix element of the Coulomb interaction  $V_C$  between the electronic parts of the states  $|D^*A\rangle$  and  $|DA^*\rangle$ . Thus the electronic transition matrix element is

$$U = \langle DA^* | V_C | D^*A \rangle = \frac{1}{R^3} \left( \mathbf{D}_D \cdot \mathbf{D}_A - \frac{3}{R^2} (\mathbf{D}_D \cdot \mathbf{R})(\mathbf{D}_A \cdot \mathbf{R}) \right), \quad (6)$$

where  $R$  is the separation between the systems, and  $D_D$  and  $D_A$  are the transition dipole moments of the donor and acceptor, respectively. We use atomic units throughout, and we assume that the dielectric constant is 1. We look in detail at specific models later, but for the moment we note that for typical systems the dipole moment is about 10 D, so at separations of around 5 nm the interaction energy  $U \sim 10^{-4}$  eV, compared to the typical energy gaps between ground and excited states of 1–2 eV.

In the absence of other effects, we could analyze the dynamics of this coupled system by restricting to the subspace spanned by the states  $|D^*A\rangle$  and  $|DA^*\rangle$  and computing the time evolution of the initial state  $|D^*A\rangle$  under the influence of the interaction  $U$ . The Hamiltonian is

$$H = \begin{pmatrix} E_1 & \bar{U}\langle f | \\ U|f\rangle & E_2 + h \end{pmatrix}, \quad (7)$$

where  $E_1$  and  $E_2$  are the electronic energy gaps of the donor and acceptor, respectively;  $U$  is the interaction matrix element defined in Eq. (6); and  $h$  is the diagonal energy operator of the continuous exciton band in the excited state. Also,  $|f\rangle$  denotes the creation operator for the exciton as in Eq. (4), and  $\langle f |$  denotes the corresponding annihilation operator.

### B. The master equation

In our model we also include the effects of fluorescent decay from the excited state to the ground state for both systems. We do this by introducing jump operators for the (irreversible) fluorescent decays from excited to ground state and use a master equation to compute the time evolution of the density matrix. So we are using the Markov approximation for the coupling to the electromagnetic field which causes fluorescence.<sup>23</sup> In order to separate the outcomes from the two excited states  $|D^*A\rangle$  and  $|DA^*\rangle$ , we use two copies of the ground state to indicate which molecule has decayed (since

the jump operators are irreversible, there is no coupling from these ground states back to the excited states). Thus the system is represented by a density matrix  $\rho$ , spanning the states  $|D^*A\rangle$ ,  $|DA^*\rangle$ ,  $|\hat{D}A\rangle$ , and  $|\hat{D}\hat{A}\rangle$ , where  $|\hat{D}A\rangle$  and  $|\hat{D}\hat{A}\rangle$  are copies of the ground state, and the two fluorescent decay channels are  $|D^*A\rangle \rightarrow |\hat{D}A\rangle$  and  $|DA^*\rangle \rightarrow |\hat{D}\hat{A}\rangle$ . In this subspace the Hamiltonian is

$$H_{DA} = \begin{pmatrix} E_1 & \bar{U}\langle f | & 0 & 0 \\ U|f\rangle & E_2 + h & 0 & 0 \\ 0 & 0 & 0 & 0 \\ 0 & 0 & 0 & 0 \end{pmatrix}. \quad (8)$$

The effects of fluorescence are implemented by the jump operators:

$$J_1 = \begin{pmatrix} 0 & 0 & 0 & 0 \\ 0 & 0 & 0 & 0 \\ 1 & 0 & 0 & 0 \\ 0 & 0 & 0 & 0 \end{pmatrix}, \quad J_{2,i} = \begin{pmatrix} 0 & 0 & 0 & 0 \\ 0 & 0 & 0 & 0 \\ 0 & 0 & 0 & 0 \\ 0 & \langle u_i | & 0 & 0 \end{pmatrix}, \quad (9)$$

where  $\{|u_i\rangle\}$  form an orthonormal basis in the exciton space. The master equation is

$$\frac{d\rho}{dt} = -i[H_{DA}, \rho] + \frac{\gamma_1}{2} (2J_1\rho J_1^\dagger - J_1^\dagger J_1\rho - \rho J_1^\dagger J_1) + \sum_i \frac{\gamma_2}{2} (2J_{2,i}\rho J_{2,i}^\dagger - J_{2,i}^\dagger J_{2,i}\rho - \rho J_{2,i}^\dagger J_{2,i}), \quad (10)$$

where  $\gamma_1$  and  $\gamma_2$  are the rates for fluorescence  $|D^*A\rangle \rightarrow |\hat{D}A\rangle$  and  $|DA^*\rangle \rightarrow |\hat{D}\hat{A}\rangle$ , respectively.

### C. Definition of the efficiency, Förster radius, and FRET rate

Using the master equation in Eq. (10), it is possible to compute the probability of exciton transfer from the donor to the receiver and to find the efficiency of this process. In the absence of FRET, the system ultimately ends up in state  $|\hat{D}A\rangle$ . Thus we define the efficiency of FRET to be the long-run probability that this does not happen; that is,

$$F = 1 - \lim_{t \rightarrow \infty} \langle \hat{D}A | \rho(t) | \hat{D}A \rangle. \quad (11)$$

The Förster radius  $R_0$  is then defined by the condition that at this separation the efficiency reaches 50%. That is,

$$R_0 = \max\{R : F \geq 0.5\}. \quad (12)$$

The FRET rate  $\gamma_{\text{FRET}}$  can also be computed from the efficiency, by comparing the rates for fluorescence of the donor and FRET:

$$\gamma_{\text{FRET}} = \gamma_1 \frac{F}{1 - F}, \quad (13)$$

where  $\gamma_1$  is the natural fluorescence rate for the donor. This follows from the relation

$$F = \frac{\gamma_{\text{FRET}}}{\gamma_{\text{FRET}} + \gamma_1}. \quad (14)$$

## IV. SOLUTION OF THE MASTER EQUATION

We solve the master equation given in Eq. (10) with the initial condition  $\rho(0) = |D^*A\rangle\langle D^*A|$ , corresponding to the

donor in its excited state and the acceptor in the ground state. The solution of Eq. (10) takes the block diagonal form,

$$\rho(t) = \begin{pmatrix} \rho_{11}(t) & \rho_{12}(t) & 0 & 0 \\ \rho_{21}(t) & \rho_{22}(t) & 0 & 0 \\ 0 & 0 & \rho_{33}(t) & 0 \\ 0 & 0 & 0 & \rho_{44}(t) \end{pmatrix}. \quad (15)$$

The top left  $2 \times 2$  block is

$$\begin{pmatrix} \rho_{11}(t) & \rho_{12}(t) \\ \rho_{21}(t) & \rho_{22}(t) \end{pmatrix} = e^{-iBt} \begin{pmatrix} 1 & 0 \\ 0 & 0 \end{pmatrix} e^{iB^*t}, \quad (16)$$

where  $B$  is the non-Hermitian operator acting on the space spanned by  $|D^*A\rangle$  and  $|DA^*(\varepsilon)\rangle$ , i.e.,

$$B = \begin{pmatrix} E_1 - \frac{i}{2}\gamma_1 & \bar{U}\langle f| \\ U|f\rangle & E_2 + h - \frac{i}{2}\gamma_2 \end{pmatrix}, \quad (17)$$

and  $|f\rangle$  is the Lorentzian function in Eq. (4). The remaining diagonal entries in Eq. (15) are given by

$$\rho_{33}(t) = \gamma_1 \int_0^t \rho_{11}(s) ds, \quad (18)$$

$$\rho_{44}(t) = \gamma_2 \int_0^t \text{Tr} \rho_{22}(s) ds. \quad (19)$$

In order to facilitate the notation, define the state

$$|\psi_0\rangle = \begin{pmatrix} 1 \\ 0 \end{pmatrix}. \quad (20)$$

It follows that the efficiency is given by

$$F = 1 - \rho_{33}(\infty) = 1 - \gamma_1 \int_0^\infty |\langle \psi_0 | e^{-iBs} | \psi_0 \rangle|^2 ds. \quad (21)$$

Thus the calculation reduces to the problem of finding matrix elements of the operator  $e^{-iBs}$ . This is straightforward because  $B$  is a rank 1 perturbation of a diagonal operator. The key step is the reduction to a related two-state system. Namely, define the  $2 \times 2$  matrix

$$\hat{B} = \begin{pmatrix} E_1 - \frac{i}{2}\gamma_1 & \bar{U} \\ U & E_2 + E_3 - \frac{i}{2}(\gamma_1 + \gamma_2) \end{pmatrix}. \quad (22)$$

It is shown in Appendix A that

$$\langle \psi_0 | e^{-iBs} | \psi_0 \rangle = \langle \psi_0 | e^{-i\hat{B}s} | \psi_0 \rangle, \quad (23)$$

and thus

$$F = 1 - \gamma_1 \int_0^\infty |\langle \psi_0 | e^{-i\hat{B}s} | \psi_0 \rangle|^2 ds. \quad (24)$$

Thus the effect of the exciton coupling in this model is the same as in a two-state model with a second channel for decay of the excited state to the ground state, at a rate which is the inverse lifetime of the exciton.

The efficiency  $F$  in (24) can be evaluated by finding the eigenvectors and eigenvalues of  $\hat{B}$ . The assumption that  $\gamma_1, \gamma_2 > 0$  implies that  $\hat{B}$  has two eigenvalues with negative imaginary parts. These can be computed explicitly, and the

initial state  $|\psi_0\rangle$  can be written as a linear combination of the eigenvectors. The result is

$$F = \frac{(1+r)|U|^2}{(1+r)^2|U|^2 + 4r\left[\frac{\Gamma^2}{16} + (E_1 - E_2 - E_3)^2\right]}, \quad (25)$$

where

$$\Gamma = \gamma_1 + \gamma_2 + \gamma \quad (26)$$

and

$$r = \frac{\gamma_1}{\gamma_2 + \gamma}. \quad (27)$$

### A. Förster radius and FRET rate

From Eq. (25) we compute the Förster radius and the FRET efficiency for this model. Setting  $F = 1/2$  we get the condition

$$|U|^2 = \frac{4r}{1-r^2} \left[ \left( \frac{\gamma_1 + \gamma_2 + \gamma}{4} \right)^2 + (E_1 - E_2 - E_3)^2 \right]. \quad (28)$$

The interaction  $U$  is given by Eq. (6). Introducing an angular factor  $\kappa$ , this gives

$$|U|^2 = \kappa^2 \frac{D_D^2 D_A^2}{R^6} \quad (29)$$

and, hence, the formula for the Förster radius,

$$R_0^6 = \frac{1-r^2}{4r} \frac{\kappa^2 D_D^2 D_A^2}{\frac{1}{16}(\gamma_1 + \gamma_2 + \gamma)^2 + (E_1 - E_2 - E_3)^2}. \quad (30)$$

### B. Exciton lifetime and scaling at resonance

At resonance where the energies match we have  $E_1 - E_2 - E_3 = 0$ . In this case we have

$$F = \frac{\gamma_2 + \gamma}{\gamma_1 + \gamma_2 + \gamma} \frac{|U|^2}{|U|^2 + \frac{\gamma_1(\gamma_2 + \gamma)}{4}}. \quad (31)$$

Define the dimensionless parameter

$$\eta = \frac{4|U|^2}{\gamma_1(\gamma_2 + \gamma)}; \quad (32)$$

then at resonance we get

$$F = \frac{\gamma_2 + \gamma}{\gamma_1 + \gamma_2 + \gamma} \frac{\eta}{\eta + 1}. \quad (33)$$

It is reasonable to expect that the inverse exciton lifetime  $\gamma$  is much larger than the fluorescence rates  $\gamma_1, \gamma_2$ . In this case the FRET efficiency at resonance takes the simple form

$$F = \frac{\eta}{\eta + 1}, \quad \eta = \frac{4|U|^2}{\gamma_1\gamma}. \quad (34)$$

This same scaling relation has been found for resonant energy transfer between classical oscillators<sup>1</sup> and seems to be a general feature of this type of phenomenon.

### C. Temperature dependence

In order to incorporate nonzero temperature effects, we introduce vibronic ground states for the acceptor, labeled  $\{|\phi_{\text{gr}}(\varepsilon_1)\rangle\}$ , where  $\varepsilon_1$  is the energy in the ground-state vibronic

band. These states are assumed nondegenerate, and thus completely labeled by their energy eigenvalue  $\varepsilon_1$ , with respect to the Hamiltonian determined by the electronic state  $|\psi_{\text{gr}}\rangle$ . Thus a general state in the acceptor band will be

$$|A\rangle = \sum_{\varepsilon_1} c(\varepsilon_1) |\phi_{\text{gr}}(\varepsilon_1)\rangle, \quad (35)$$

with the normalization condition  $\sum_{\varepsilon_1} |c(\varepsilon_1)|^2 = 1$ . The vibronic Hamiltonian is diagonal in this representation, and so the time evolution of a state is

$$|A\rangle \rightarrow \sum_{\varepsilon_1} c(\varepsilon_1) e^{-i\varepsilon_1 t} |\phi_{\text{gr}}(\varepsilon_1)\rangle. \quad (36)$$

To include nonzero temperatures, we assume a Boltzmann distribution for the initial equilibrium state; that is,

$$\rho_{\text{eq}} = Z^{-1} \sum_{\varepsilon_1} e^{-\varepsilon_1/k_B T} |\phi_{\text{gr}}(\varepsilon_1)\rangle \langle \phi_{\text{gr}}(\varepsilon_1)|. \quad (37)$$

We then compute the thermal average of the efficiency over initial vibronic energies. Thus the temperature-dependent efficiency is

$$F(T) = Z^{-1} \sum_{\varepsilon_1} e^{-\varepsilon_1/k_B T} F(\varepsilon_1) d\varepsilon_1, \quad (38)$$

where  $F(\varepsilon_1)$  is given by Eq. (25) with  $E_1$  replaced by the initial energy  $E_1 + \varepsilon_1$ . By using this formula for  $F(\varepsilon_1)$  we assume that initially the acceptor is in a pure vibronic ground state  $|\phi_{\text{gr}}(\varepsilon_1)\rangle$ , which transitions to the exciton state  $f(\varepsilon)$  due to the FRET interaction. Our main simplification is the following: we assume that the reverse operation causes a transition from the exciton state back to the *same initial vibronic state*  $|\phi_{\text{gr}}(\varepsilon_1)\rangle$ . So under this reverse operation an exciton state  $\psi(\varepsilon)$  is mapped to  $\alpha |\phi_{\text{gr}}(\varepsilon_1)\rangle$ , where the amplitude is  $\alpha = \int \overline{f(\varepsilon)} \psi(\varepsilon_2) d\varepsilon$ . Thus the acceptor always returns to its initial ground state (this assumption has also been made for exact calculations of coherent exciton scattering).<sup>24</sup>

Carrying out the summation in Eq. (38) requires knowledge of the phonon spectrum of the acceptor, and we do not pursue the question further here. However, we note that this effect of the temperature is expected to be small because at room temperature  $k_B T$  is significantly smaller than the energy scale given by  $\gamma \sim 0.1$  eV.

## V. COMPARISON WITH STANDARD FRET FORMULAS

The standard Förster formulas for FRET rate and Förster radius involve the overlap integral between the normalized donor fluorescence spectrum and the acceptor absorption spectrum. The formula for the Förster radius (in cm) is<sup>8</sup>

$$R_F^6 = \frac{9000 \ln(10) \kappa^2 Q_D}{128 \pi^5 N_A} J, \quad (39)$$

where  $Q_D$  is the donor quantum yield,  $N_A$  is Avogadro's number, and  $J$  is the overlap integral (in  $\text{cm}^3 \text{dm}^3/\text{mol}$ ),

$$J = \int_0^\infty \varepsilon_A(\lambda) F_D(\lambda) \lambda^4 d\lambda \quad (40)$$

(recall that we have assumed that the refractive index is 1). Here  $F_D(\lambda)$  is the donor emission spectrum [normalized so that  $\int_0^\infty F_D(\lambda) d\lambda = 1$ , where  $\lambda$  is the wavelength (in cm)],

and  $\varepsilon_A$  is the molar absorption coefficient (in  $\text{cm}^{-1} \text{dm}^3/\text{mol}$ ). Inserting values for the constants gives

$$R_F^6 = 8.79 \times 10^{-25} Q_D \kappa^2 J. \quad (41)$$

In our two-level model the donor is assumed to have a narrow band fluorescence spectrum centered at energy  $E_1$ , so the overlap integral is essentially  $\varepsilon_A(\lambda) \lambda^4$  evaluated at the wavenumber  $\lambda = 2\pi c/E_1$ . Thus the formula is

$$R_F^6 = 8.79 \times 10^{-25} Q_D \kappa^2 \varepsilon_A(2\pi c/E_1) (2\pi c/E_1)^{-4}. \quad (42)$$

The acceptor's molar absorption coefficient can be evaluated from the standard absorption rate for the transition from ground state to excited state, using Fermi's Golden Rule to compute the rate. The details are carried out in Appendix B and the result (in  $\text{cm}^{-1} \text{dm}^3/\text{mol} = 10 \text{ m}^2/\text{mol}$ ) is

$$\frac{\varepsilon_A \ln(10)}{N_A a_B^2} = \frac{2\pi}{\omega c} \frac{10 E_2^2 D_A^2 \gamma}{(\omega - E_2 - E_3)^2 + \gamma^2/4}, \quad (43)$$

where  $a_B$  is the Bohr radius. Using this expression for the absorption coefficient in Eq. (39) and setting  $\omega = E_1$ , we get (in a.u.)

$$R_F^6 = 9 \kappa^2 Q_D \left(\frac{c}{E_1}\right)^3 \frac{\gamma D_A^2}{(E_1 - E_2 - E_3)^2 + \gamma^2/4} \left(\frac{E_2}{E_1}\right)^2. \quad (44)$$

Turning now to our Eq. (30), we use the Einstein A coefficient to relate the fluorescence rate and the dipole strength of the donor:

$$\gamma_1 = \frac{4 E_3^3}{3 c^3} D_D^2. \quad (45)$$

This approximation for  $\gamma_1$  given by Eq. (45) neglects spectral shifts and broadening. Thus our expression for  $R_0$  becomes

$$R_0^6 = \frac{3}{16} (1 - r^2) \kappa^2 \left(\frac{c}{E_1}\right)^3 \times \frac{(\gamma_2 + \gamma) D_A^2}{(E_1 - E_2 - E_3)^2 + (\gamma_1 + \gamma_2 + \gamma)^2/16}. \quad (46)$$

Comparing Eq. (46) and Eq. (44), we see that our result differs from the standard one in several ways. In particular, the width of the Lorentzian is  $(\gamma_1 + \gamma_2 + \gamma)/4$  instead of  $\gamma/2$ , and the factor  $(E_2/E_1)^2$  is absent in Eq. (46). However, for realistic models we expect that  $\gamma \gg \gamma_1, \gamma_2$ , hence  $r \ll 1$ . So when we compare the values at the resonant energy (where  $E_1 - E_2 - E_3 = 0$ ), and if we set  $Q_D = 1$ , then we get the ratio

$$\frac{R_0}{R_F} = 0.7783 \left(\frac{E_1}{E_2}\right)^{1/3}. \quad (47)$$

We expect that  $E_3 \simeq E_2/10$  (the energy difference between the donor's emission peak and the acceptor's absorption peak), and thus  $E_1/E_2 \simeq 1.11$ , so we find a quite close agreement with the standard result.

## VI. APPLICATION: QUANTUM DOTS AND BACTERIORHODOPSIN

Recent proposals for improved dye-sensitized solar cells<sup>25,26</sup> involve replacing the liquid dye by nanoparticles

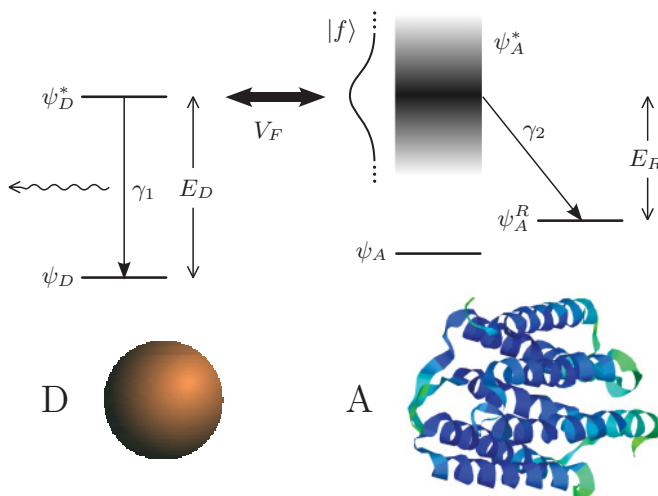


FIG. 1. (Color online) Schematics of the continuum model for FRET. The donor is a quantum dot, while the acceptor is an optoelectric protein such as bacteriorhodopsin.

attached to a substrate and exploiting FRET to achieve efficient energy transfer.<sup>27</sup> One candidate material is a mixture of QDs and the protein bR.<sup>28–30</sup> In one scenario the QD would act as an antenna for photon absorption, with subsequent transfer to the retinal complex in bR. The retinal complex in bR is known to be an efficient absorber of photons through direct capture, and this same efficiency is expected for nonradiative transfer of excitons from QD to bR via the FRET mechanism.<sup>4</sup> The methods developed in this paper can be used to evaluate the efficiency of FRET in this hybrid system. The QD has a band gap of approximately 2 eV (depending on its diameter),<sup>31,32</sup> and after photon absorption it rapidly relaxes to its lowest energy excited state, thus the QD is well modeled as a two-state system.

In its ground state the retinal molecule has a planar conformation. Upon excitation it briefly enters a band of planar excited states (due to an electronic transition consistent with the Franck-Condon principle) and then rapidly relaxes to a nonplanar conformation.<sup>33</sup> The latter transition occurs within a few hundred femtoseconds, is effectively irreversible, and thus signals the transfer of the excitation to bR. The planar excited state lies in a band of closely spaced levels corresponding to different vibrational and rotational states. Recent studies have demonstrated that coherence persists in the exciton state for several hundred femtoseconds after initial excitation.<sup>33</sup>

Our model QD/bR is schematized in Fig. 1 and it is a simplified version of the more general model described above. The values of the various parameters can be obtained from known properties of the molecules. The wave function  $f$  has the Lorentzian form, centered at the exciton energy  $E_3$ . We assume transfer on resonance, so that  $E_1 = E_2 + E_3 = 2$  eV. The width  $\gamma$  is the inverse lifetime of the exciton, which is known from coherence analysis to be at least 100 fs, so  $\gamma$  is upper bounded by around 0.05 eV. The rate  $\gamma_1$  is set by the QD experimental lifetime,<sup>32</sup> so  $\gamma_1^{-1} = 16$  ns, and the rate  $\gamma_2^{-1} = 500$  fs.<sup>33</sup> However, they are not important in the calculations since they are much smaller than  $\gamma$ . The FRET

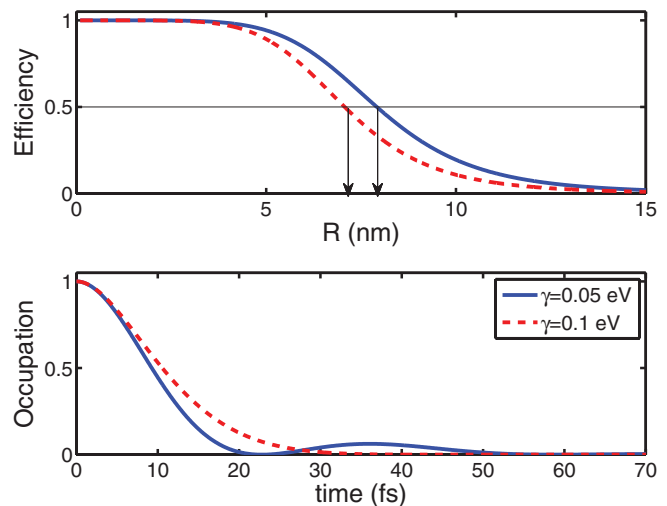


FIG. 2. (Color online) (a) Efficiency for QD-bR as a function of separation; (b) occupation probability of initial excited state as a function of time. Arrows show the position of  $R_0$  for two values of  $\gamma$ .

coupling strength  $U$  is determined by the formula<sup>16</sup>

$$U = \frac{\kappa D_{\text{QD}} D_{\text{bR}}}{\epsilon_r R^3}, \quad (48)$$

where  $\epsilon_r$  is the permittivity of the medium,  $R$  is the separation between the molecules,  $D_{\text{QD}}$  and  $D_{\text{bR}}$  are the dipole moments of the QD and bR, respectively, and the angular factor  $\kappa$  depends on the orientations of dipoles relative to the separation between molecules. We use the values  $D_{\text{QD}} = D_{\text{bR}} = 10$  D,  $\epsilon_r = 1$  (permittivity of medium, assumed dry), and  $\kappa = 1$  and keep the separation distance  $R$  as a free parameter. In atomic units this gives

$$U = \frac{15.479}{R^3}. \quad (49)$$

Figure 2(a) shows the efficiency as a function of  $R$  for these values. The FRET distance  $R_0$  is consistent with the one estimated from experiments of about 7–8 nm.<sup>30</sup> The curve almost exactly matches the phenomenological formula<sup>6–8</sup> for efficiency  $E = R_0^6 / (R_0^6 + R^6)$ . Figure 2(b) shows the occupation probability of the initial donor excited state as a function of time, for the same parameter values and with a separation  $R = 2$  nm. Coherent oscillations are apparent if  $\gamma = 0.05$  eV.

## VII. CONCLUSIONS

We have introduced an exactly solvable model for FRET, which captures the key features of Förster's electronic-excitonic coupling in a microscopic quantum mechanical setting. The standard Förster equations are accurate when the following conditions are satisfied.<sup>6</sup>

(a) The dipole-dipole approximation for the electronic coupling can be employed appropriately for the donor-acceptor interaction.

(b) Interactions among donors or acceptors and static disorder effects leading to spectral line broadening can be neglected.

(c) The energy transfer dynamics is incoherent.

Our approach goes at least beyond condition c since, at short distances and times, the formalism is able to capture the coherent energy transfer. The model uses a master equation with Lindblad operators to take account of fluorescence and relaxation effects and uses a continuum of excited states in the acceptor to implement the exciton dynamics. The model is robust and can easily be extended to include more complicated exciton dynamics. As a concrete application the model is used to analyze FRET coupling between a QD and bR, where it makes realistic predictions of the FRET distance.

#### ACKNOWLEDGMENTS

We are grateful to Nicolas Bouchonville, Michael Molinari, and Paul Champion for useful discussions. B.B. was supported by US Department of Energy, Office of Science, Basic Energy Sciences Contract Nos. DE-FG02 07ER46352 and DE-FG02-08ER46540 (CMSN) and benefited from the allocation of supercomputer time at NERSC and Northeastern University's Advanced Scientific Computation Center (ASCC). V.R. was supported by the NSF, the Wallace H. Coulter Foundation, USAFOSR, the ONR, the NIH, and Harvard Medical School. V.R. acknowledges the Rothschild Foundation and Varun for providing support.

#### APPENDIX A

We use resolvent techniques to compute the exponential of  $B$ . Recall the resolvent representation

$$e^{-iBs} = \frac{1}{2\pi i} \oint e^{-izs} (z - B)^{-1} dz, \quad (\text{A1})$$

where the line integral encloses the spectrum of  $B$  in the complex plane. The assumption that  $\gamma_1, \gamma_2 \geq 0$  implies that  $B$  has no spectrum in the upper half-plane, so the resolvent  $(z - B)^{-1}$  is analytic in the upper half-plane. There is a cut along the real axis where the spectrum of  $h_2$  lies, and also, possibly, poles in the lower half-plane. The line integral encloses the cut and also any poles in the lower half-plane. In the lower half-plane the integration contour can be deformed to a large semicircle  $z = Re^{-i\theta}$  with  $0 \leq \theta \leq \pi$ . For  $s > 0$  the contribution of this semicircle vanishes in the limit  $R \rightarrow \infty$ , thus for  $s > 0$  the line integral in Eq. (A1) can be written as

$$\begin{aligned} e^{-iBs} &= -\frac{1}{2\pi i} \int_{-\infty+i\epsilon}^{\infty+i\epsilon} e^{-izs} (z - B)^{-1} dz \\ &= \frac{1}{2\pi i} \int_{-\infty+i\epsilon}^{\infty+i\epsilon} e^{-izs} (B - z)^{-1} dz. \end{aligned} \quad (\text{A2})$$

This leads to the formula

$$\langle \psi_0 | e^{-iBs} | \psi_0 \rangle = \frac{1}{2\pi i} \int_{-\infty+i\epsilon}^{\infty+i\epsilon} e^{-izs} \langle \psi_0 | (B - z)^{-1} | \psi_0 \rangle dz. \quad (\text{A3})$$

We next derive an explicit formula for the matrix element  $\langle \psi_0 | (B - z)^{-1} | \psi_0 \rangle$  appearing on the right-hand side above, under the assumption that  $\text{Im}z > 0$ . Define

$$(B - z)^{-1} = \begin{pmatrix} I_{11}(z) & I_{12}(z) \\ I_{21}(z) & I_{22}(z) \end{pmatrix}. \quad (\text{A4})$$

Then the Feshbach method yields  $I_{11}(z)$ ,

$$\langle \psi_0 | (B - z)^{-1} | \psi_0 \rangle = \left( E_1 - \frac{i}{2} \gamma_1 - z - |U|^2 M \right)^{-1}, \quad (\text{A5})$$

where

$$M = \langle f | \left( E_2 + h - \frac{i}{2} \gamma_2 - z \right)^{-1} | f \rangle. \quad (\text{A6})$$

Using the Lorentzian form for  $f$  and the diagonal energy operator  $h$ , the matrix element  $M$  is

$$\begin{aligned} M &= \frac{\gamma}{2\pi} \int_{-\infty}^{\infty} \frac{1}{k - E_3 + \frac{i}{2} \gamma} \frac{1}{k - E_3 - \frac{i}{2} \gamma} \\ &\quad \times \frac{1}{E_2 + k - \frac{i}{2} \gamma_2 - z} dk. \end{aligned} \quad (\text{A7})$$

This integral may be computed by completing the contour in the lower half-plane and evaluating the sum of the residues. For  $\text{Im}z > 0$  this gives

$$M = \frac{1}{E_2 + E_3 - \frac{i}{2}(\gamma + \gamma_2) - z}. \quad (\text{A8})$$

Inserting this into Eq. (A5) leads to the expression

$$I_{11}(z) = \left( E_1 - \frac{i}{2} \gamma_1 - z - \frac{|U|^2}{E_2 + E_3 - \frac{i}{2}(\gamma + \gamma_2) - z} \right)^{-1}. \quad (\text{A9})$$

The key observation now is that Eq. (A9) is the resolvent of the reduced two-state system defined by the matrix introduced in Eq. (22); that is,

$$\hat{B} = \begin{pmatrix} E_1 - \frac{i}{2} \gamma_1 & \bar{U} \\ U & E_2 + E_3 - \frac{i}{2}(\gamma + \gamma_2) \end{pmatrix}. \quad (\text{A10})$$

It follows that

$$\langle \psi_0 | (B - z)^{-1} | \psi_0 \rangle = \langle \psi_0 | (\hat{B} - z)^{-1} | \psi_0 \rangle, \quad (\text{A11})$$

and hence we obtain for all  $s$

$$\langle \psi_0 | e^{-iBs} | \psi_0 \rangle = \langle \psi_0 | e^{-i\hat{B}s} | \psi_0 \rangle. \quad (\text{A12})$$

#### APPENDIX B

The acceptor's molar absorption coefficient can be computed by using the following time-dependent Hamiltonian for the electronic transition in the presence of a classical field:

$$H(t) = \begin{pmatrix} E_2 & \nu e^{-i\omega t} \\ \bar{\nu} e^{i\omega t} & 0 \end{pmatrix}. \quad (\text{B1})$$

Here  $E_2$  is the energy of the excited state,  $\omega$  is the frequency of the radiation, and  $\nu$  is the coupling between the field and the system. This coupling is given by

$$\nu = \frac{ie}{mc} \int \bar{\psi}_{\text{exc}}(r) (\mathbf{A}_0 \cdot \nabla) \psi_{\text{gr}}(r) d^3r, \quad (\text{B2})$$

where  $\psi_{\text{exc}}$  and  $\psi_{\text{gr}}$  are the excited- and ground-state wave functions, and  $\mathbf{A}_0$  is the field strength (assumed constant). We have used the rotating-wave approximation and dropped

the counter-rotating term proportional to  $e^{i\omega t}$ . Standard dipole approximations lead to

$$v = -\frac{i}{c} |\mathbf{A}_0| E_2 D_A. \quad (\text{B3})$$

The radiation intensity (power per unit area) is related to the field strength through the time-averaged Poynting vector, and this gives

$$I_{\text{in}} = \frac{\omega^2 |\mathbf{A}_0|^2}{2\pi c}. \quad (\text{B4})$$

Combining the electronic transition rate with the exciton amplitude, Fermi's Golden Rule gives the following rate for transitions in this radiation field:

$$\sigma = 2\pi |v|^2 |f(\omega - E_2)|^2. \quad (\text{B5})$$

The absorption coefficient determines the rate of energy absorption by an ensemble of molecules. Consider a slab of absorber with unit cross-sectional area and thickness  $x$ ,

illuminated by light of frequency  $\omega$  and intensity  $I_{\text{in}}$ . Then the output intensity is given by the Beer-Lambert law,

$$I_{\text{out}} = I_{\text{in}} 10^{-\epsilon_A k x}, \quad (\text{B6})$$

where  $\epsilon_A$  is the molar absorption coefficient and  $k$  is the concentration (in moles per unit volume). The number of molecules in the slab is  $N_A k x$ , where  $N_A$  is Avogadro's number. The energy absorbed per unit time by transitions is thus  $N_A k x \sigma \omega$ . Equating this to the energy difference between input and output gives the result in atomic units:

$$\begin{aligned} \epsilon_A \ln(10) &= \frac{N_A \sigma \omega}{I_{\text{in}}} \\ &= \frac{N_A \omega 2\pi |v|^2 |f(\omega - E_2)|^2}{I_{\text{in}}} \\ &= \frac{2\pi}{\omega c} \frac{N_A E_2^2 D_A^2 \gamma}{(\omega - E_2 - E_3)^2 + \gamma^2/4}. \end{aligned}$$

\*king@neu.edu

<sup>1</sup>A. Kurs, A. Karalis, R. Moffatt, J. D. Joannopoulos, P. Fisher, and M. Soljacic, *Science* **317**, 8386 (2007).

<sup>2</sup>S. Mukherjee, M. P. Nadesalingam, P. Guagliardo, A. D. Sergeant, B. Barbiellini, J. F. Williams, N. G. Fazleev, and A. H. Weiss, *Phys. Rev. Lett.* **104**, 247403 (2010).

<sup>3</sup>A. Vittorini-Orgeas and A. Bianconi, *J. Supercond. Novel Magn.* **22**, 215 (2009).

<sup>4</sup>J. I. Basham, G. K. Mor, and C. A. Grimes, *ACS Nano* **4**(3), 1253 (2010).

<sup>5</sup>Y. Liu, M. A. Summers, C. Edder, J. M. J. Frechet, and M. D. McGehee, *Adv. Mater.* **17**, 2960 (2005).

<sup>6</sup>G. D. Scholes, *Annu. Rev. Phys. Chem.* **54**, 57 (2003).

<sup>7</sup>R. M. Clegg, in *Laboratory Techniques in Biochemistry and Molecular Biology*, Vol. 33, edited by T. W. J. Gadella (Academic Press, Burlington, MA, 2009), pp. 1–57.

<sup>8</sup>T. Förster, *Naturwissenschaften* **33**, 166 (1946).

<sup>9</sup>Electronic excitation transfer (EET) is another term used in the literature to describe the transfer of energy via nonradiative dipole coupling.

<sup>10</sup>J. Perrin, *C. R. Acad. Sci. (Paris)* **184**, 1097 (1927).

<sup>11</sup>V. May and O. Kühn, *Charge and Energy Transfer Dynamics in Molecular Systems* (Wiley-VCH, Weinheim, 2004).

<sup>12</sup>G. W. Robinson and R. P. Frosch, *J. Chem. Phys.* **38**, 1187 (1963).

<sup>13</sup>Th. Förster, in *Delocalized Excitation and Excitation Transfer*, edited by O. Sinnanoglu, Vol. 3 (Academic Press, New York, 1965), pp. 93–137.

<sup>14</sup>J. Roden, A. Eisfeld, W. Wolff, and W. T. Strunz, *Phys. Rev. Lett.* **103**, 058301 (2009).

<sup>15</sup>A. Ishizaki and G. R. Fleming, *J. Chem. Phys.* **130**, 234111 (2009).

<sup>16</sup>B. W. Lovett, J. H. Reina, A. Nazir, and G. A. D. Briggs, *Phys. Rev. B* **68**, 205319 (2003).

<sup>17</sup>S. K. Sekatskii, M. Chergui, and G. Dietler, *Europhys. Lett.* **63**, 21 (2003).

<sup>18</sup>D. Hofmann, T. Körzdörfer, and S. Kümmel, *Phys. Rev. A* **82**, 012509 (2010).

<sup>19</sup>J. S. Briggs and A. Eisfeld, *Phys. Rev. E* **83**, 051911 (2011).

<sup>20</sup>E. N. Zimanyi and R. J. Silbey, *J. Chem. Phys.* **133**, 144107 (2010).

<sup>21</sup>G. S. Engel, T. R. Calhoun, E. L. Read, T.-K. Ahn, T. Mancal, Y.-C. Cheng, R. E. Blankenship, and G. R. Fleming, *Nature* **446**, 782 (2007).

<sup>22</sup>J. Jortner, *Pure Appl. Chem.* **27**, 389 (1971).

<sup>23</sup>The only information about the fluorescence spectrum needed in the present model is the rate of fluorescence given by the jump operator. This rate can be obtained from experiments.

<sup>24</sup>J. Roden, G. Schulz, A. Eisfeld, and J. Briggs, *J. Chem. Phys.* **131**, 044909 (2009).

<sup>25</sup>E. W. McFarland and J. Tang, *Nature* **421**, 616 (2003); M. Grätzel, *ibid.* **421**, 586 (2003).

<sup>26</sup>S. W. H. Eijt, P. E. Mijnders, L. C. van Schaarenburg, A. J. Houtepen, D. Vanmaekelbergh, B. Barbiellini, and A. Bansil, *Appl. Phys. Lett.* **94**, 091908 (2009).

<sup>27</sup>E. T. Hoke, B. E. Hardin, and M. D. McGehee, *Opt. Express* **18**, 3893 (2010).

<sup>28</sup>R. Li, C. M. Li, H. Bao, and Q. Bao, *Appl. Phys. Lett.* **91**, 223901 (2007).

<sup>29</sup>A. Rakovich, A. Sukhanova, N. Bouchonville, M. Molinari, M. Troyon, J. H. M. Cohen, Y. Rakovich, J. F. Donegan, and I. Nabiev, *Proc. SPIE* **7366**, 736620 (2009); N. Bouchonville, M. Molinari, A. Sukhanova, M. Artemyev, V. A. Oleinikov, M. Troyon, and I. Nabiev, *Appl. Phys. Lett.* **98**, 013703 (2011).

<sup>30</sup>M. H. Griep, K. A. Walczak, E. M. Winder, D. R. Lueking, and C. R. Friedrich, *Biosens. Bioelectron.* **25**, 1493 (2010).

<sup>31</sup>M. H. Weber, K. G. Lynn, B. Barbiellini, P. A. Sterne, and A. B. Denison, *Phys. Rev. B* **66**, 041305(R) (2002).

<sup>32</sup>S. A. Crooker, J. A. Hollingsworth, S. Tretiak, and V. I. Klimov, *Phys. Rev. Lett.* **89**, 186802 (2002).

<sup>33</sup>V. I. Prokhorenko, A. M. Nagy, S. A. Waschuk, L. S. Brown, R. R. Birge, and R. J. D. Miller, *Science* **313**, 1257 (2006); M. Chergui, *ibid.* **313**, 1246 (2006).